Nature-Inspired Self-Powered Sensors and Energy Harvesters

Sengupta, Debarun; Chen, Ssu-Han; Kottapalli, Ajay Giri Prakash

Published in:
Self-Powered and Soft Polymer MEMS/NEMS Devices

DOI:
10.1007/978-3-030-05554-7_3

Chapter 3
Nature-Inspired Self-Powered Sensors and Energy Harvesters

Debarun Sengupta, Ssu-Han Chen, and Ajay Giri Prakash Kottapalli

3.1 Introduction

Biomimetic and nature-inspired design philosophies have been gaining popularity among modern researchers for past few decades. During product development, efficient design is the key to enhancing the performance of the device. For example, while designing a locomotive, a key concern is to have an overall aerodynamic architecture to reduce air resistance. There are many other examples we might find in daily life where design might be of utmost importance. Living creatures have evolved over the ages through the process of natural selection to adapt to their surrounding environment. Taking inspiration from living beings to solve engineering problems is often the best design approach as it saves a lot of time in design optimization. For example, the sophisticated sensing capabilities demonstrated by the aquatic creatures make use of complex biological sensors having multilayered functionalities.

D. Sengupta
Department of Advanced Production Engineering, Engineering and Technology Institute Groningen (ENTEG), Faculty of Science and Engineering, University of Groningen, Groningen, The Netherlands

S.-H. Chen
Microsystems Research, School of Electrical Engineering and Telecommunications, The University of New South Wales, Kensington, Australia

A. G. P. Kottapalli (✉)
Department of Advanced Production Engineering, Engineering and Technology Institute Groningen (ENTEG), Faculty of Science and Engineering, University of Groningen, Groningen, The Netherlands

MIT Sea Grant College Programme, Massachusetts Institute of Technology (MIT), Cambridge, MA, USA
e-mail: a.g.p.kottapalli@rug.nl

A. G. P. Kottapalli et al., *Self-Powered and Soft Polymer MEMS/NEMS Devices*, SpringerBriefs in Applied Sciences and Technology,
https://doi.org/10.1007/978-3-030-05554-7_3

With the rapid growth of semiconductor industry for past two decades, there has been tremendous growth in the field of semiconductor sensor technologies. Development of micro/nano-fabrication techniques has led to the increase of micro/nano-system-based sensors like pressure sensors, heat sensors, and flow sensors.

With the demand in market for wearable and other consumer electronics devices, the focus of the industry is now to develop state-of-the-art sensors capable of carrying out sensing tasks at low-power budget. This is where the philosophy of bioinspiration can play an essential role by virtue of having nature evolved clever design concept tailored to a sensing task.

The sensing capabilities demonstrated by underwater creatures have drawn the interests of engineers and material scientists for last three decades. Significant research efforts have been put in to understand the sensing principles employed by aquatic creatures to navigate in turbid underwater environments. Design and development of efficient self-powered sensors are the primary motivation behind understanding the sensing principles, morphologies, and functionalities of various natural sensors found in underwater animals.

3.1.1 Flow Sensing in Marine Creatures

Evolution has led to the development of some of the most impressive flow sensing capabilities in underwater creatures. For surviving in harsh underwater environments full of predators, fishes have evolved with sensors capable of sensing flows accurately. Many marine animals are capable of detecting prey and predators by forming a three-dimensional map of their surrounding by sensing velocity and pressure field surrounding them [1]. This is achieved by employing an array of flow sensors distributed along their bodies.

For example, blind cave fishes living in dark caves lack vision and yet are capable of generating a three-dimensional map of their habitat by sensing pressure and velocity variation in their immediate surroundings [2, 3]. This sophisticated hydrodynamic sensing is achieved by employing an array of sensors also known as neuromasts embedded into their lateral lines.

Crocodiles are known for employing dome-shaped pressure receptors which are capable of sensing surface waves generated due to the tiniest drop of water. By doing so crocodiles can orient themselves to surface waves in complete darkness [4].

Another interesting example is of the harbor seals utilizing their whiskers to sense wake signatures left by the prey up to 30 s after it has already passed. Their whiskers are sensitive enough to detect a flow having a magnitude as low as 245 μm s^{-1} [5].

3.1.2 Flow Sensing in Fishes

The lateral line in a fish consists of an array of sensors known as neuromasts. They are pressure-gradient sensors capable of sensing slightest perturbance in the flow fields surrounding the fish due to the presence of any obstacles or objects. Fishes

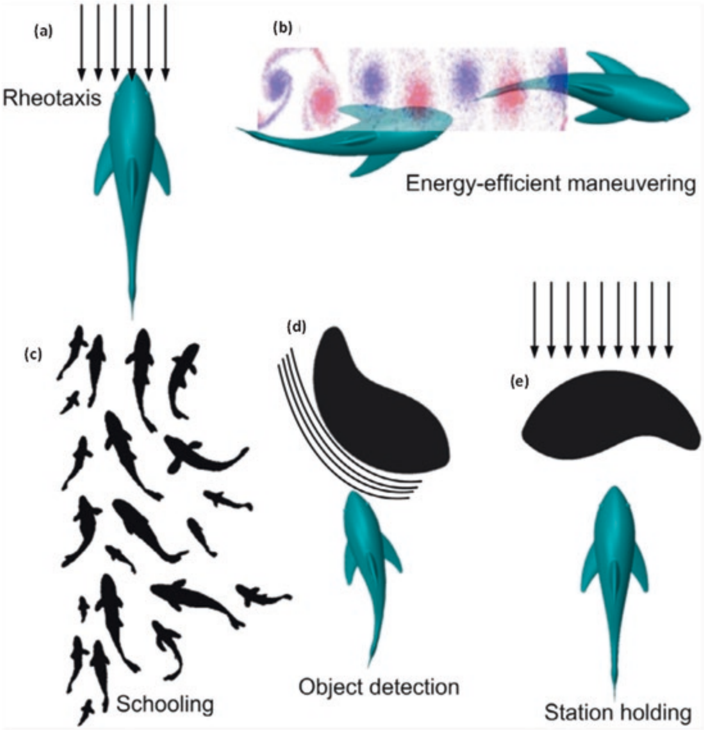

Fig. 3.1 Schematic diagram showing various lateral-line mediated behavior demonstrated by fishes. (Figure reproduced from [12] with permission of ©IOPSCIENCE)

demonstrate a range of behavior mediated by lateral-line including rheotaxis, energy-efficient maneuvering, schooling, object detection, and station holding [6–11]. Figure 3.1 is a schematic representation of some of the interesting lateral-line mediated behavior observed in fishes.

Lateral-line systems (LLS) are of utmost importance in blind cave fishes (Fig. 3.2a) as they depend on them for sensing the surroundings. Due to their functional significance, the LLS in fishes are sometimes referred to as "touch at a distance" [13]. As stated earlier, LLS comprise of the smallest sensory unit known as neuromasts which in turn consists of hair cells, stereocilia bundles, kinocilium, and nerves. The neuromast with stereocilia bundles is encapsulated by an elongated or dome-shaped structure made of a soft porous gel-like material called as cupula.

Depending on their location, neuromasts can be classified into two categories:

- Superficial neuromasts (SNs): This type of neuromast is present on the surface of the fish skin.
- Canal neuromasts (CNs): This type of neuromast is present below the surface of the skin embedded in fluid-filled canals (Fig. 3.2c). The canal opens up on both ends, to the skin water interface by means of pores.

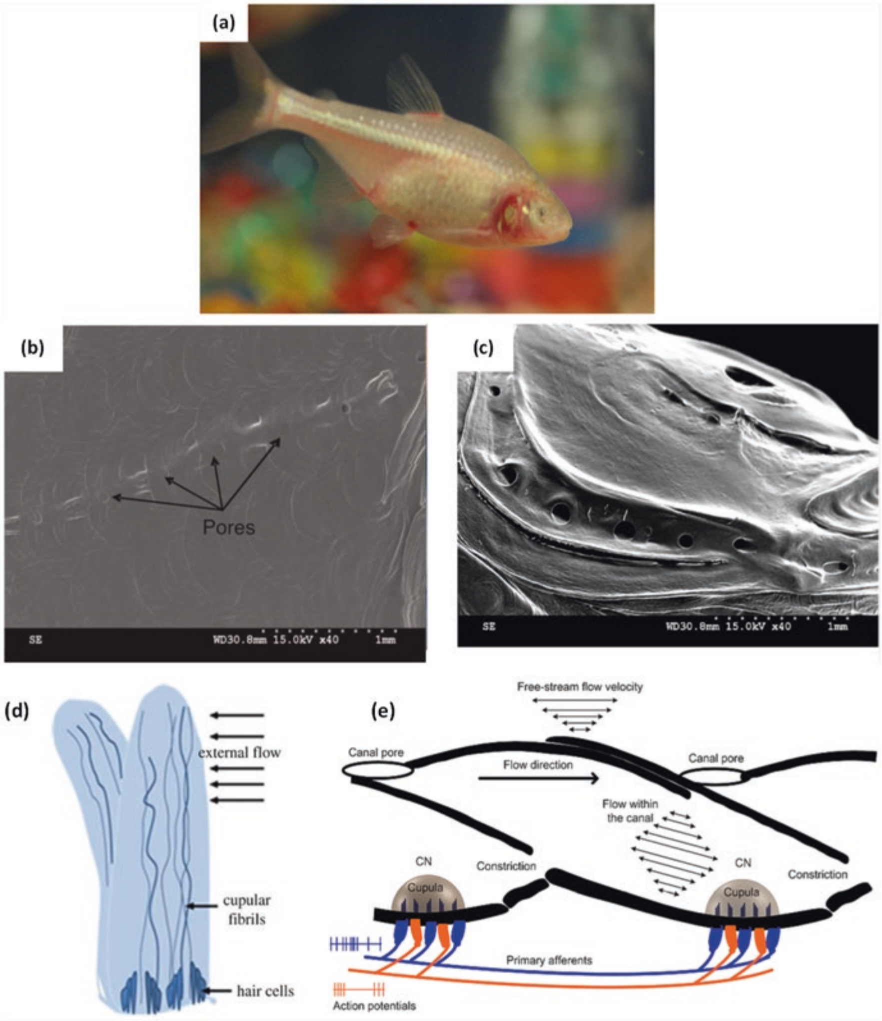

Fig. 3.2 (**a**) Image of a blind cave fish [17]. (**b**) SEM micrograph showing the lateral line found in cave fishes. (Figure reproduced from [18] with permission of ©Sagepub). (**c**) SEM images showing the canal pores of CNs [19]. (**d**) Schematic diagram showing the structure of an SN and explaining its working principle [19]. (**e**) Schematic diagram showing the structure of a CN and explaining its working principle [19]

The main differences between SNs and CNs lie in the structure of their cupula and stereocilia. SNs have an elongated cupula with an elongated tip (Fig. 3.2d), whereas the cupulae found in CNs are dome-shaped (Fig. 3.2e). The elastic modulus of cupula of SN (10 Pa) is significantly lower than that of cupula of CN having an elastic modulus of 10 kPa [14–16]. Both CNs and SNs are characterized by two spatially intermingled and oppositely oriented groups of hair cells.

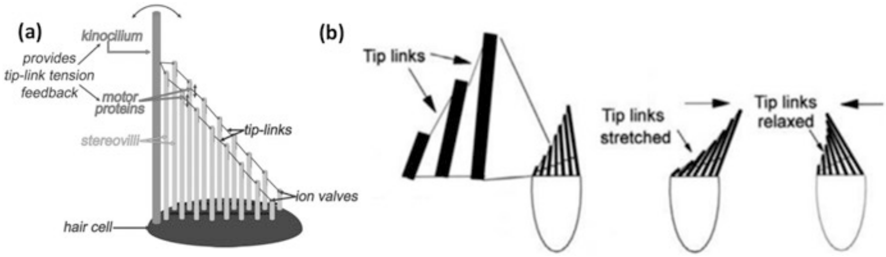

Fig. 3.3 (**a**) Schematic representation of hair cell structure comprising kinocilium and stereocilia. (Figure reproduced from [22] with permission of WILEY-VCH.) (**b**) Schematic representation of stretching and relaxing of tip links in stereocilia leading to excitatory and inhibitory response of neuromasts. (Figure reproduced from [23] with permission of Elsevier Inc.)

The sensing mechanism of SN is fundamentally different from CN. The water which flows past the skin of the fish interacts with the SNs generating responses proportional to the velocity of the water flow. In case of the CNs, the water entering a canal through the skin pores interacts with the sensors generating responses which are proportional to the net acceleration of the water flow [20, 21].

Figure 3.3a shows the schematic diagram of hair cell having stereocilia and kinocilium. Water interacting with the cupula deflects it which starts the transduction process involving inhibition or excitation through mechanically sensitive ion channel. Tip links connect the stereocilia at their tips (Fig. 3.3a). Figure 3.3b presents the bending of stereocilia toward or away from kinocilium causing stretching/relaxation of the tip links. When the stereocilia are bent, the tip links are either stretched or relaxed depending on the direction of the bending of the stereocilia. When stereocilia bend toward the long kinocilium, the tip links are stretched leading to the initiation of the transport of ions across the hair cell membrane [23, 24]. Bending of stereocilia in the opposite direction leads to relaxation of the tip links causing prevention of ion transport. The responses in intermediate directions are cosine functions of input directions.

Due to the structural differences in SNs and CNs, they respond differently to different frequency domains. SNs are like low-pass filters which react to low-frequency stimuli, whereas the CNs behave like high-pass filters responding to stimuli in the higher-frequency domain [11, 23]. Combining both SNs and CNs, fishes can filter out low-frequency noises from high-frequency large amplitude signals, thus improving the overall signal-to-noise ratio.

3.1.3 Flow Sensing in Crocodiles

Crocodiles achieve passive sensing through mechanoreceptors called integumentary sensory organs (ISOs) [25]; they are sometimes known as dome pressure receptors (DPRs) [4]. These receptor organs are densely populated on the jaws and the

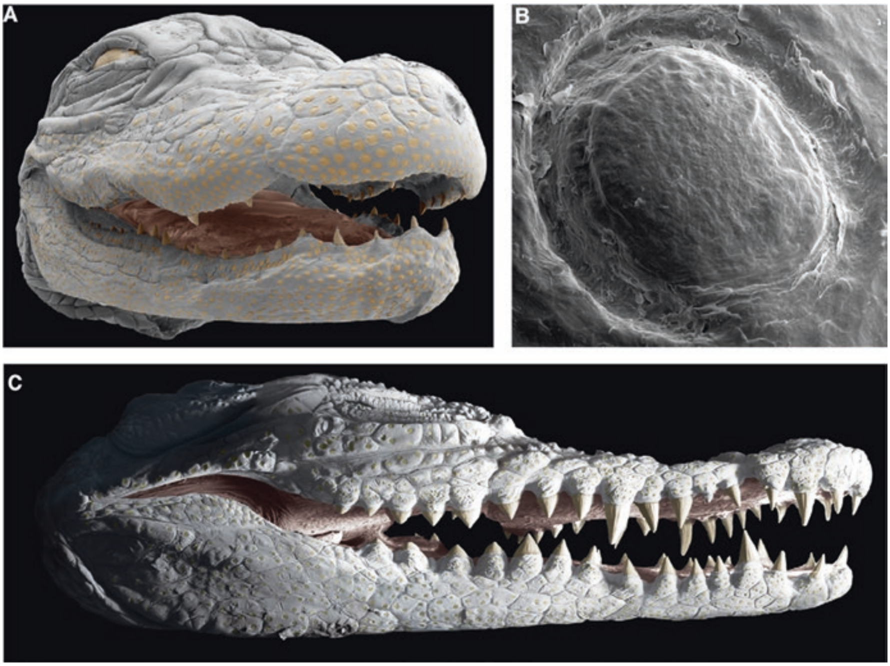

Fig. 3.4 Cranial region of a crocodilian viewed under the scanning electron microscope with false colorization: (**a**) the cranial region of an alligator with ISOs (yellow) shown, (**b**) a single ISO of an alligator shown at higher magnification, (**c**) the cranial region of a crocodile with distributed ISO shown (yellow). (Figure reproduced from [25] with permission of Journal of Experimental Biology)

rest of the body of the crocodile with dome-shaped structures varying from 0.2 to 1.2 mm in diameter [25], as shown in Fig. 3.4a–c. The ISOs consist of slowly adapting (SA) and rapidly adapting (RA) receptors which enable crocodiles to locate the source of disturbances both on the surface of the water and underwater to hunt for preys in dark and murky environments. These mechanoreceptors are categorized into two types of receptor cells – (i) SA receptors are associated with Merkel cells [25] which respond to constant intensity level of stimulus; (ii) RA receptors are related to lamellated corpuscles [25] which react to a change in the intensity level of the stimulus.

The response of the SA receptors to a square wave stimulus and that of RA receptors to a sinusoidal stimulus has been demonstrated by Leitch et al. [23]. From the response of the two stimulus signals, it can be verified that the SA receptors responded throughout the presence of the steady intensity level of the stimulus and the RA receptors responded to the same frequency as that of the sinusoidal stimulus. With these distinct response characteristics, the SA receptors are well suited for sensing steady flows or variations, whereas RA receptors are more suitable for sensing oscillatory pressures caused by fast-moving aquatic animals.

3.1.4 Flow Sensing in Harbor Seals

Several species of marine mammals have evolved in nature with highly efficient hydrodynamic sensory systems. For example, harbor seals use their whiskers (vibrissae) to track prey, evade predators, and identify conspecifics (Fig. 3.5a). In the natural habitat, it is crucial for the seals to have this ability to track the hydrodynamic trail of the fish to capture the swimming directions of their prey. Dehnhardt et al. have demonstrated a "go" and "no-go" testing paradigm on a trained blindfolded and acoustically masked harbor seal (*Phoca vitulina*) that restricted the seal to utilize its whiskers to detect flows. They identified that relying on whiskers, the seal is capable of detecting subtle water movements as low as 245 μm/s in the 10–100 Hz range [26]. When the cross-sectional shape of the whiskers has a close resemblance to a bluff body (cylindrical shape), the wake forms a double array of staggered vortices, known as the Kármán street. The trembling forces as a result of Kármán street act on the body with an amplitude comparable to its cross-sectional dimension and with high frequency. Such vibration also referred to as vortex-induced vibration (VIV) gives rise to oscillations in the cross-flow direction in which the corresponding flow profiles appear unsteady [27]. Remarkably, seal vibrissae are sensitive enough to detect minute changes in the flow left by marine animals while rejecting this self-induced flow noise. This noteworthy feat gives credit to the uniquely shaped whiskers with a variable cross section in the shape of an ellipsoid (Fig. 3.5b) [28]. In the spanwise direction, the geometry of the whisker varies sinusoidally, while the upstream undulation is in out of phase with the downstream undulation. With the specialized undulatory morphology, it is believed that the self-induced noise from VIV is suppressed due to this factor. These undulations are understood to disrupt the formation of Kármán vortex and cause the formation of streamwise vorticity, hence reducing substantially the fluid forces on the whisker [29]. At steady velocity, it is believed this feature allows the seal to move forward

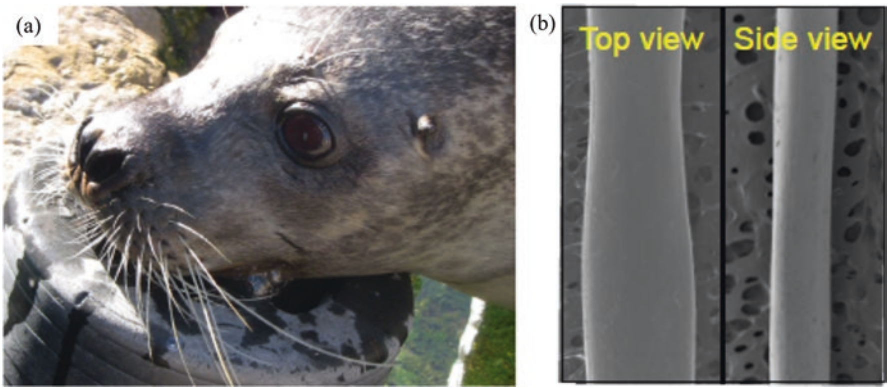

Fig. 3.5 (**a**) A harbor seal displaying its vibrissae, (**b**) SEM images of a whisker showing its undulatory, elliptical geometry. (Figure reproduced from [28] with permission of IEEE)

with minimal self-induced noise from VIV. However, seals following the trails of fish experience a more complex phenomenon. The body and caudal fin from a fish generate coherent ring-link vortical structures that induce a jet flow, as well as a drag wake, and it is only in the very far field when the two cancel each other for a self-propelled body. These wakes show predominance flow similar to that of a Kármán street, but the vortices rotate in opposite direction. Hence, understanding the hydrodynamic properties of fish detection by harbor seal whiskers can be modeled by the interaction between the wake of an upstream cylinder and a seal whisker to provide principal mechanisms that enable the fine sensitivity of the whiskers [30]. This undulation feature of the whiskers has been adopted by some biomimetic engineers in creating enhanced sensors to detect flow disturbances, which will be discussed in Sect. 3.2.3.

3.2 Underwater Animal-Inspired Self-Powered Sensors

Marine creatures have developed highly efficient sensory systems for their survival in harsh marine habitat. Engineers have taken inspiration from nature in replicating mechanoreceptors for applications in autonomous underwater vehicles (AUVs) and efficient flow sensors. These nature-inspired sensors provide passive sensing techniques that are, in comparison, more efficient than active sensing strategies. Due to this reason, scientists and engineers have taken great initiative in understanding how the sensory organs of the marine creatures have help them to avoid predators and hunt for preys.

In this section, various sensing techniques inspired by marine creatures like fish, crocodiles, and harbor seals are presented. The neuromasts from fishes have been studied extensively in the past and have been mimicked for various sensing applications. Integumentary sensory organs (ISOs) found in crocodiles are excellent receptors to detect steady-state pressures and oscillatory pressures under water. These receptors are replicated by engineers with MEMS technology to perform the same functionalities. Vibrissae organs are integral to harbor seals to navigate through water and sense hydrodynamic information when they are visually or acoustically impaired. The whiskers of the harbor seal have the ability to detect low fluid velocities in low-frequency range. Engineers have adapted this concept in reproducing artificial whiskers to sense minute disturbances in water.

3.2.1 Neuromast-Inspired Biomimetic MEMS Sensors

The fish LLS has inspired researchers in recent years to develop biomimetic MEMS sensors. Efforts have been put in to separately develop SN- and CN-inspired sensors for different sensing applications. The most widely reported artificial hair cell-based flow sensor designs are characterized by high aspect-ratio pillar-like structures on

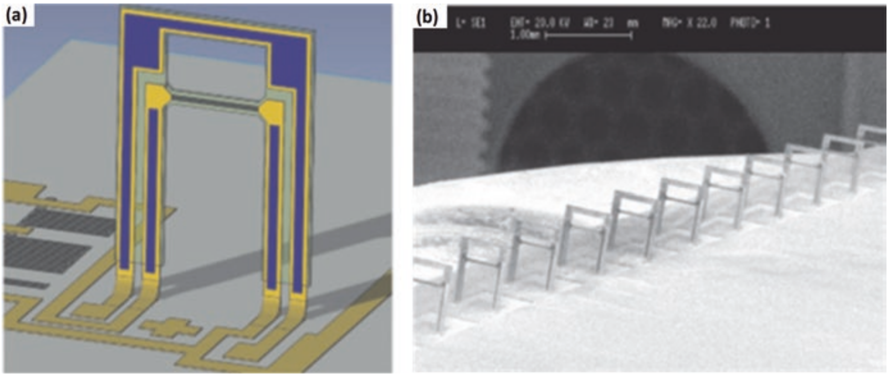

Fig. 3.6 (**a**) Schematic representation of individual microfabricated out-of-plane artificial hair cell sensors. (**b**) Scanning electron microscope image of artificial lateral line with 16 sensors spaced 1 mm apart. (Figure reproduced from [31], Copyright (2006) National Academy of Sciences, USA)

substrates known as the cilium. The structural configuration of such sensors allows for a densely packed array of sensors which pose minimum intrusion to the flow field. The critical concern while developing such sensors for the underwater environment is that they should be able to survive in the harsh marine environment irrespective of the fabrication method being employed to create such sensors.

In one of the early works, Yang et al. reported a hot wire anemometer (HWA) principle-based LLS comprising of a linear array of flow sensors, similar to the array of neuromasts found in fishes [25]. In this work, they used a unique microfabrication process combining an efficient three-dimensional assembly technique with traditional surface micromachining method to develop an array of novel hot-wire anemometer. The individual structure of each sensor consists of a 400 μm long hot wire element made of nickel filament sandwiched between two layers of polyimide which is elevated 600 μm out of the plane by two prongs (Fig. 3.6a). The nickel hot wire was reported to have a temperature coefficient of resistance of 4100 ppm/°C. The array of sensors consisted of 16 sensors with an intersensor spacing of 1 mm (Fig. 3.6b). For parallel data acquisition and noise-floor reduction, each sensor was integrated with monolithically integrated metal-oxide semiconductor circuitry. The testing of the array of sensors revealed a nonlinear characteristic in a water channel with flow velocities up to 0.25 m/s. This work demonstrated the potential of biomimetic flow sensing in an underwater environment. The authors were able to show the ability of their sensor in dipole source localization, hence discerning the dipolar near field generated by any nearby object.

Though this work was one of the firsts to show that artificial lateral line can successfully perform hydrodynamic wake detection and dipole source localization, the sensors demonstrated in the work differed from its real biological equivalent in many ways. The main difference between this artificial lateral line and real LLS is that the real LLS consist of both CNs and SNs, and each neuromast has a cupula encapsulating a bundle of hair cells, whereas the artificial lateral line only has a certain number of HWAs placed superficially.

In another work, Chen et al. developed biological hair cell-inspired artificial hair cell (AHC) sensor comprising of a high-aspect-ratio cilium structure attached at the distal end of a silicon cantilever beam [32]. The main sensing element in this AHC is a piezoresistive silicon strain gauge at the base of the cantilever. The cilium structure was made of SU-8 and was up to 700 μm in height. The sensor was reported to have high sensitivity and directionality. On subjecting to oscillatory (ac) flows generated with a dipole setup, the sensor was able to respond to velocity amplitudes as low as 0.7 mm/s. The angular resolution for the wind-tunnel directionality test was reported as 2.16°.

Building on previous works, Peleshenko et al. developed a hybrid design combining hard and soft materials to develop AHC sensor having cupula like encapsulating structure. The sensor design in the work comprised of a silicon cantilever membrane with 600 μm tall SU-8 pillar. To mimic the cupula, a viscous hydrogel synthesized by means of photopatterned polymerization of polyethylene glycol (PEG) was drop casted to form a dome shape over the SU-8 (Fig. 3.7a). The drop casting was followed by cross-linking and swelling in water at ambient conditions.

Both of the sensors with and without cupula were subjected to steady and oscillatory flows in underwater environment. The sensor with cupula demonstrated

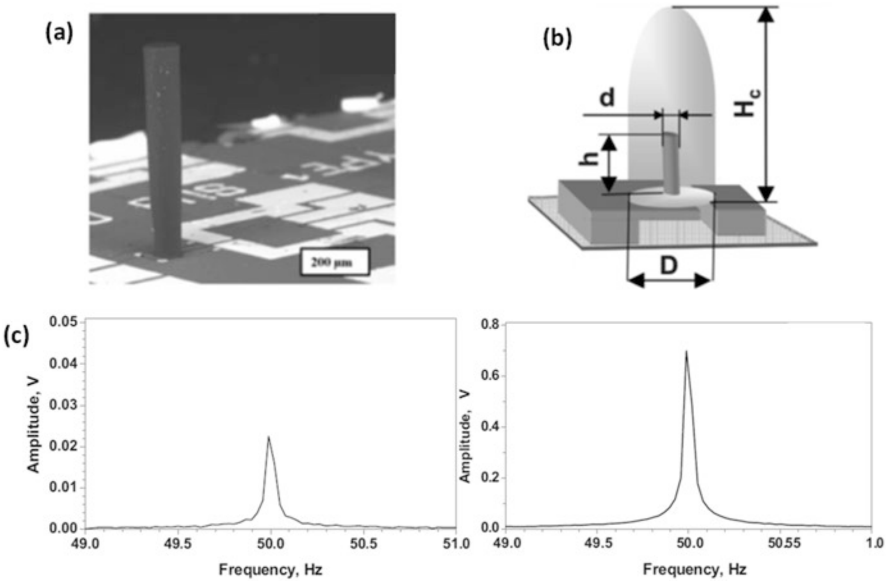

Fig. 3.7 (**a**) SEM image of the artificial hair cell-based flow sensors without hydrogel cupula. (**b**) Schematic diagram of the artificial hair cell sensor with hydrogel cupula. (**c**) Plot comparing the response of the naked hair cell sensor with the hydrogel-capped sensor subjected to 50 Hz oscillatory flow. (Figure reproduced from [14] with permission of WILEY-VCH Verlag GmbH and Co. KGaA, Weinheim)

10–30 times the signal intensity than the naked hair cell design. For a 50 Hz oscillatory flow signal, the sensor with PEG hydrogel cupula demonstrated significantly better performance than its naked counterpart (Fig. 3.7c). Also, the hydrogel cupula improved the overall minimum velocity detection threshold by 2.5 times (from 0.2 mm s^{-1} to 0.075 mm s^{-1}).

Recently, Bora et al. reported the development of MEMS-based CN-inspired self-powered sensor and demonstrated its capability of indirectly detecting steady-state flow by employing the principle of vortex-induced vibrations (VIV) [33]. The sensor reported in this work consists of three distinct parts (Fig. 3.8a, b):

1. Piezoelectric sensing element: A membrane fabricated using lead zirconate titanate (PZT) was used as the main sensing element.
2. The hair cell structure: A high aspect ratio cylindrical pillar of copper (Cu) placed in the middle of the PZT membrane was used for mimicking the tall hair cell structure. This cu pillar interacts with the fluid flow and detects disturbances in the fluid.
3. Hydrogel cupula: To mimic the dome-shaped cupula of the CNs, hyaluronic acid (HA) modified with methacrylic anhydride (MA) was drop cast over the cu pillar.

Figure 3.9a, b shows the CN-inspired sensor with and without hydrogel cupula.

The main problem with all piezoelectric sensors is electron discharging when subjected to static forces. In this work, an innovative approach to solve the problem associated with electron discharging was proposed. Vibration of the PZT membrane caused by the VIV generated on the Cu pillar is used for determination of the flow

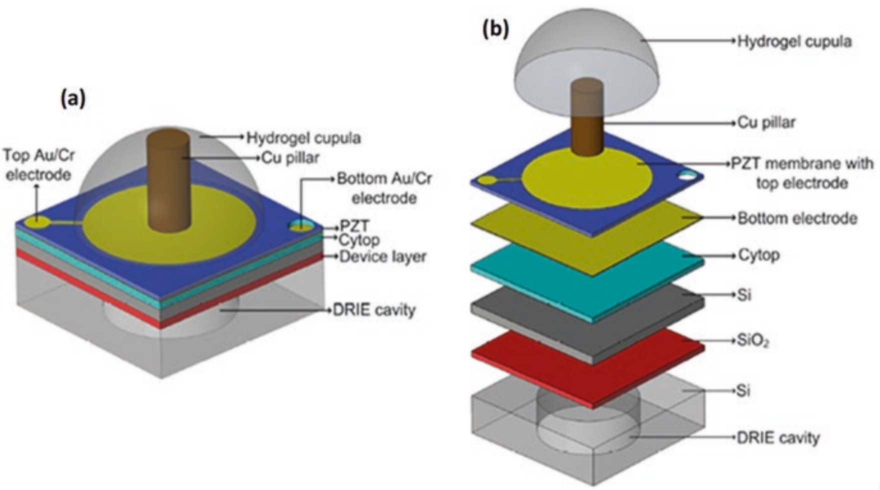

Fig. 3.8 (**a**) Schematic diagram of CN-inspired flow sensor with HA-MA hydrogel cupula. (**b**) Exploded schematic view of CN-inspired flow sensor with HA-MA hydrogel cupula. (Figure reproduced from [33] with permission of AIP)

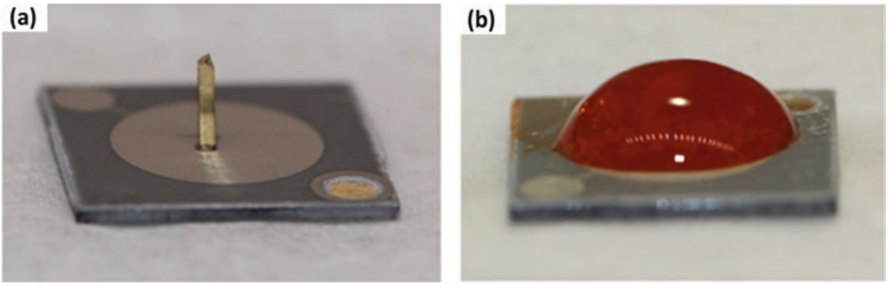

Fig. 3.9 (**a**) Photograph of the naked sensor. (**b**) Photograph of the sensor with cupula. (Figure reproduced from [33] with permission of AIP)

velocity (U). Steady-state flow sensing test was conducted on the sensor for a range of velocities (0–0.7 m/s). Figure 3.10a shows the sensor output for a steady-state flow velocity of 0.625 m/s. Oscillatory flow tests were performed on the sensor by using a vibrating sphere (dipole) to agitate the water surrounding the sensor. The dipole was driven by a series of sinusoidal signals in a plane perpendicular to the axis of the Cu pillar. The response of the sensor closely followed the driving frequency of the dipole (Fig. 3.10c). Experiments to demonstrate the advantage of having a hydrogel cupula as opposed to the naked pillar revealed a performance improvement of 2.1 times when subjected to an oscillatory flow test (at 35 Hz) (Fig. 3.10b).

3.2.2 Crocodile-Inspired Self-Powered Sensors

Autonomous underwater vehicles (AUVs) are integral instruments when it comes to underwater exploration, surveying, and military applications. In order to achieve autonomous maneuvers, the AUVs must be equipped with sensing elements to perceive their surrounding environments and enhance navigation control. Traditionally, this has been achieved by active sensing strategies like sound navigation and ranging (SONAR) and optical imaging [34]. Even though sonar technology is the most mature and adapted method for detecting the underwater environments for AUVs, it comes with inherent issues like sonar blind zones [35] and poses fatal threats to aquatic lives due to its intense sound waves transmitted by the sonar system. For optical imaging, the reliability of the environmental mapping relies on the visibility of the water [31]. Moreover, with active sensing strategies, the equipment accompanied with the sensors adds weight to the AUVs, making them energy inefficient. However, the aforementioned drawbacks can be overcome with passive sensing technologies.

By taking inspiration from the sensory organs of the crocodiles, implementing passive sensing in AUVs could potentially be possible by mimicking the ISOs of the crocodiles. Biomimetic engineers have attempted to recreate the SA and RA

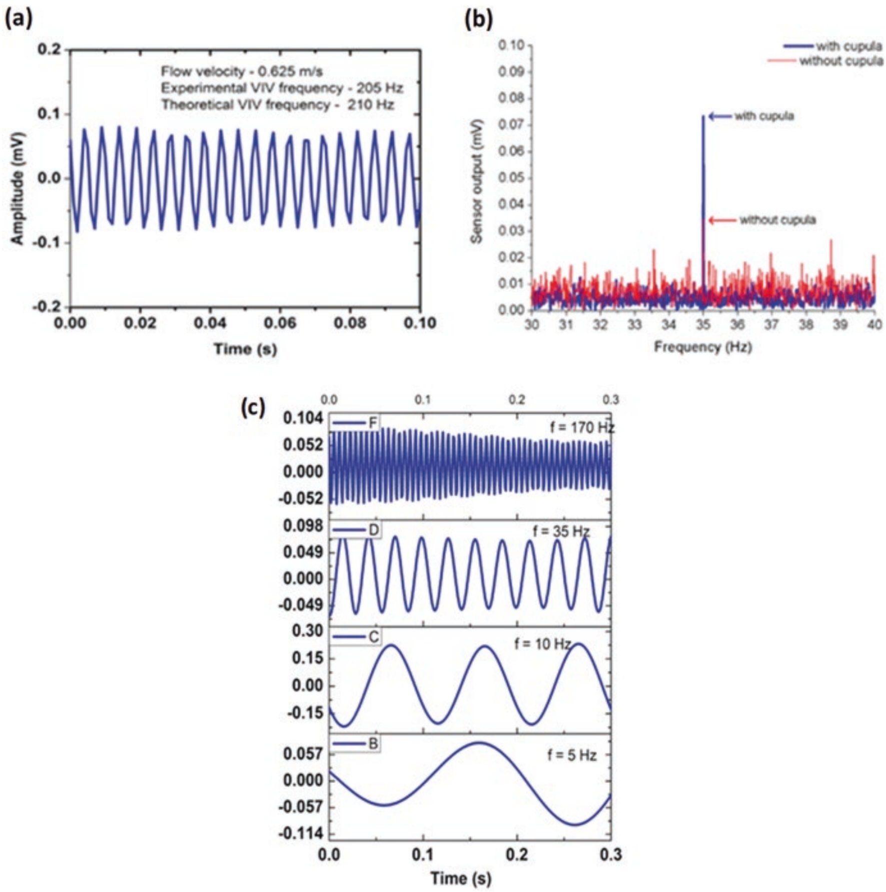

Fig. 3.10 (**a**) Response of the sensor for a steady-state flow velocity of 0.625 m/s. (**b**) Comparing the responses of the sensors with and without cupula. (**c**) Oscillatory flow responses of the sensors at various frequencies. (Figure reproduced from [33] with permission of AIP)

receptors with MEMS-based sensors [36]. The SA and RA dome-shaped receptors are constructed with piezoresistive sensors to sense steady pressures and piezoelectric sensors to sense oscillating pressures, respectively (Fig. 3.11a, b). The SA and RA domes consist of five MEMS piezoresistive pressure sensors and five MEMS piezoelectric pressure sensors, mounted on a 3D-printed polymer dome (Fig. 3.11c, d).

The replicas of the dome-shaped receptors of the ISOs on crocodiles are advantageous to sense information in three dimensions due to its spherically symmetric structure. From the patterns and combinations of the pressure value readings by the individual sensors, locating the originality of the disturbance can be determined. From experimental results by Kanhere et al. [36], the ability of SA and RA dome

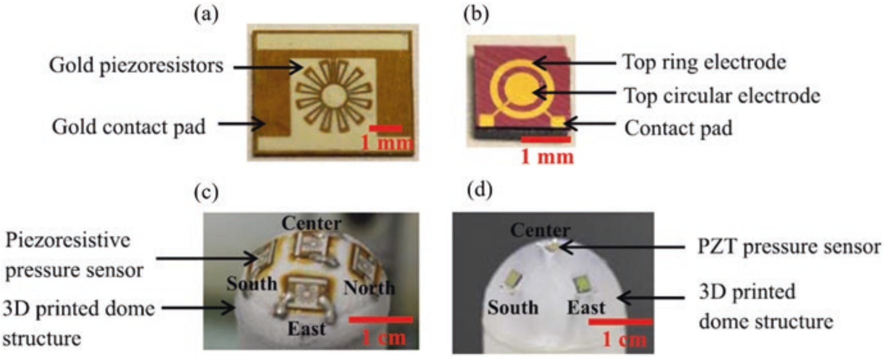

Fig. 3.11 Bioinspired MEMS SA and RA dome receptors: (**a**) piezoresistive gold sensor on LCP membrane, (**b**) micro-diaphragm piezoelectric pressure sensor, (**c**) SA dome with piezoresistive pressure sensors, (**d**) RA dome with piezoelectric pressure sensors. (Figure reproduced from [36] with permission of IOP publishing)

receptors to distinguish the direction of steady-state flows and oscillatory disturbances by determining the outputs of the five pressure sensors on each dome has been demonstrated.

3.2.3 Harbor Seal-Inspired Biomimetic Sensors

AUVs not only reply on sensing elements to perceive their surrounding environments but also determining fluid flow to aid in navigation is also crucial for autonomous control. Various commercial and military applications rely on fluid flow information to interpret target movements in water. Several researches have acquired their inspiration from harbor seals in developing highly sensitive artificial whiskers to detect hydrodynamic trails. The harbor seal can respond to extremely weak hydrodynamic stimuli with their whiskers as aforementioned. This has sparked many interests in mimicking whisker-like sensors to detect fluid motion for various applications [37–40].

A capacitive-based whisker-like sensor for fluid motion sensing has been demonstrated by Stocking et al. [37]. The sensor features a rigid artificial whisker mounted on a cone-in-cone parallel-plate capacitor base which are separated into four quadrants to provide directional information for the fluid flow. The gap between the electrodes is filled with silicone oil to obtain a dielectric constant of about 2.5. The damping and restoring force of the artificial whisker are provided by a 200 μm thick polydimethylsiloxane (PDMS) membrane, as shown in Fig. 3.12a, b. The sensor has demonstrated the ability to distinguish flow-induced forces for both steady and oscillatory conditions with millinewton-level precision. The output signal from each of the quadrants allowed the interpretation of flow direction. However, achiev-

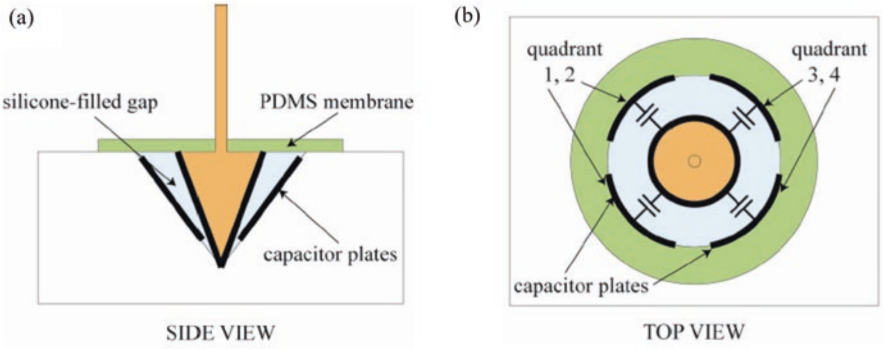

Fig. 3.12 Schematic drawings of the cone-in-cone sensor design: (**a**) side view of the sensor, (**b**) top view of the sensor. (Figure reproduced from [37] with permission of IEEE)

ing a similar sensitivity among the quadrants is particularly challenging with this design due to the requirement for the inner cone to be perfectly aligned to the outer cone. The same group later presented a Wake Information Detection and Tracking System (WIDTS) with an array of eight capacitive-based whisker-like sensors developed from their previous work [41]. The individual sensors in the WIDTS are designed to measure the direction and speed of fluid motion. As a proof of concept, the WIDTS has been fitted to a trained harbor seal via a bite plate to hold securely in the mouth of the seal. The WIDTS is then exposed to a hydrodynamic path left by a miniaturized submarine guided by the tracking behavior of the seal. This provided a realistic sensing environment for the WIDTS to detect underwater disturbances similar to the environment encountered by the seal. From observing the tracking path of the seal, the WIDTS also demonstrated detection of the hydrodynamic disturbances triggered by the variations of the seal's tracking behavior. This provided evidence that the artificial whisker arrays may achieve underwater sensing capabilities.

Alternative whisker-like sensors have been proposed by Alvarado et al. [39, 40]. The design has a more close resemblance to that of a whisker follicle sinus complex system (FSC). Figure 3.13a illustrates the major structural components inside the follicle sinus complex and a simple mechanical model of the whisker-follicle system. Figure 3.13b outlines the basic whisker sensor design. The whisker with length $L+\ell$ is supported by a viscoelastic membrane which mimics the FSC. Inside the sensor capsule are four flexible displacement sensors to detect whisker base oscillations θ in two perpendicular plans of motion (along and across the direction of motion). The flexible sensors consist of commercially available piezoresistive-based sensors, Bend Sensor®, that changes its electrical conductivity as it is bent (http://www.flexpoint.com/). The viscoelastic membranes used are silicone-based rubbers with mechanical properties close (Young's modulus and viscosity) to that of FSC tissues (Ecoflex 0010, Ecoflex 0030, and MoldMax 30) (http://www.smooth-on.com).

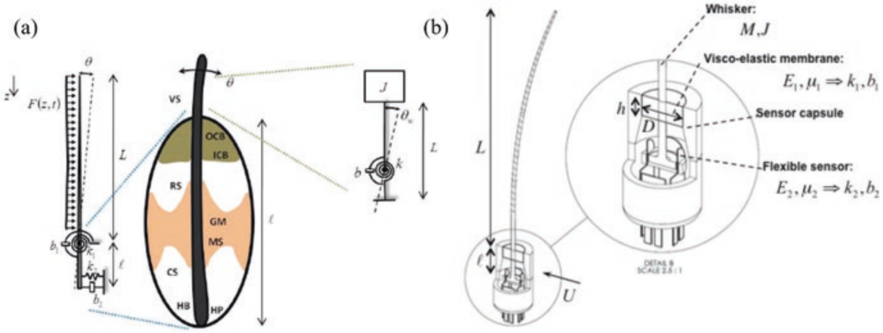

Fig. 3.13 (**a**) Whisker-FSC system and a simple lumped parameter model. (**b**) Basic whisker-like sensor design. (Figure reproduced from [40] with permission of IEEE)

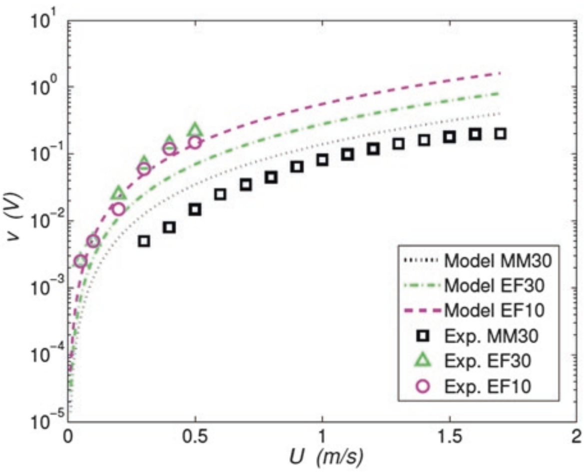

Fig. 3.14 Whisker as velocity sensor. Measured sensor voltage v vs. towing speed U for three different silicone-based rubbers with different mechanical properties vs. predicted performances based on derived model in [40]. (Figure reproduced from [40] with permission of IEEE)

The whisker-like sensors have been tested in water by fixing the whisker modules on a carriage and towed at constant speeds along a 10 m × 2 m × 1.5 m water tank. The sensors are capable of detecting flow speeds spanning from 0.05 m/s up to 2 m/s with a whisker length L of 0.17 m, as shown in Fig. 3.14. With mindful design considerations, the artificial FSC can be tailored to sense a wide range of velocities for specific applications.

The aforementioned whisker-like sensors employ cylindrical standing pillars or strands to mimic the whiskers of the harbor seals. When these artificial whiskers are subjected to flow disturbances, vortex-induced vibration other than drag pressure are induced by the steady flow. The whiskers in seals have developed unique geometry along the length of their whiskers which is believed to have an important role in suppressing vortex-induced vibrations [29]. More recently, bioinspired artificial

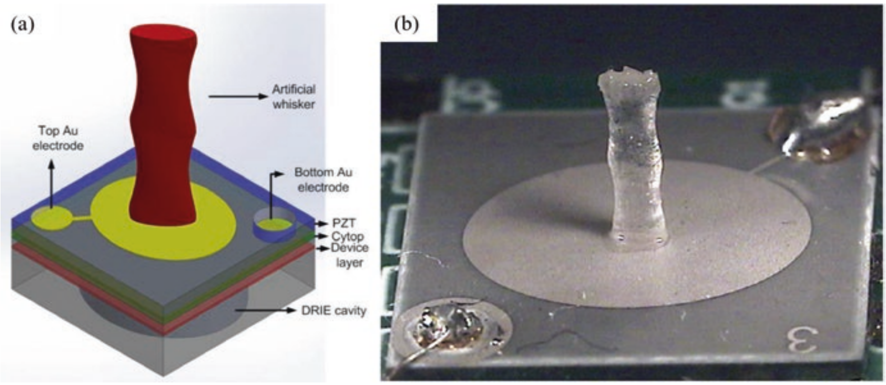

Fig. 3.15 (**a**) Schematic of the micro-whisker sensor (**b**) fabricated device with the artificial polymer micro-whisker fabricated by stereolithography mounted at the center of the PZT membrane. (Figure reproduced from [42] with permission of IEEE)

whisker fabricated by stereolithography (SLA) coupled with a piezoelectric MEMS sensing membrane has been demonstrated with the capability to suppress vortex-induced vibrations (Fig. 3.15a) [42, 43]. The micro-pillar mimicking the real seal whisker is fabricated from a UV curable Si60 polymer material with a high-resolution VIPER™ SLA® system. The varying spatial features are formed layer by layer with SLA processing techniques. The piezoelectric sensing diaphragm is formed by bonding a bulk PZT plate to an SOI wafer using spun-on Crypto as an intermediate layer. The PZT plate is flanked by two Cr/Au metal electrodes that form as the contact pads to sense the output piezoelectric voltages. The sensing membrane is released from the backside by DRIE. Figure 3.15b shows the sensing device with the micro-pillar mounted at the center of the PZT membrane.

The performance of the sensor is evaluated using a vibrating sphere stimulus in a water tank. The threshold and sensitivity of the sensor is tested by varying the amplitude of the sinusoidal signal supplied to the dipole. The output signal from the sensor is amplified by a gain of 500, and the resultant peak-to-peak signal amplitudes from various oscillatory flow velocities are illustrated in Fig. 3.16a. The sensor demonstrated a linear response up to an oscillatory flow velocity of 250 mm/s, with a lowest detectable velocity of 193 μm/s. The capability to suppress vortex-induced vibrations in low flow velocities due to the whisker-like undulations of the micro-pillar is demonstrated by comparing to a cylindrical micro-pillar in a steady-state flow. The two types of sensors are tested in a water tunnel with the water flow in perpendicular to the long axis of the micro-pillars. The vortex-induced vibrations for the cylindrical and undulated micro-pillars are shown in Fig. 3.16b, c, respectively. From observation, the vortex-induced vibration frequency peak in case of the whisker-like design is 50 times smaller than that of the cylindrical design.

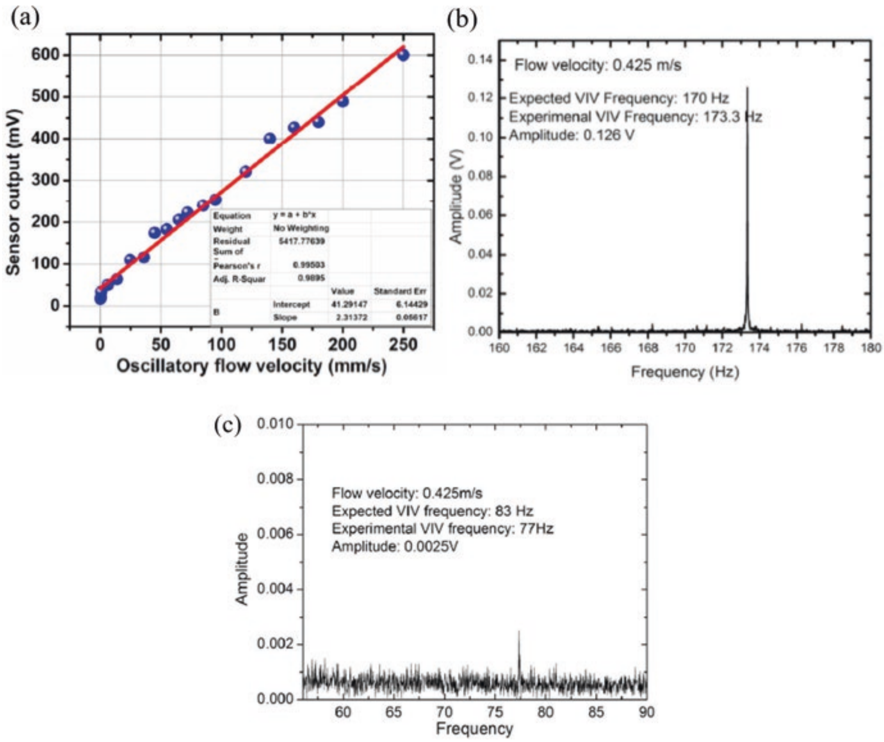

Fig. 3.16 (**a**) Oscillatory flow velocity sensor output. (Figure reproduced from [42] with permission of IEEE), (**b**) vortex-induced vibration frequency of a cylindrical micro-pillar design, (**c**) vortex-induced vibration frequency of a whisker-like undulated design. (Figures reproduced from [43] with permission of IEEE)

3.3 Conclusions and Future Work

Survival hydrodynamics among underwater animals have long inspired scientists and engineers to develop efficient nature-inspired sensors for sensing tasks in underwater vehicles. In particular, the sensing systems in fishes like SNs and CNs are capable of sensing slightest of changes in pressure and velocity. Using their LLs, fishes are capable of generating a three-dimensional map of their surroundings which help them in navigating and complex maneuvering. In this work, we have reviewed some of the most relevant works focused on underwater creature-inspired biomimetic sensors for various flow sensing applications.

The mechanoreceptors of crocodiles can be an inspiration for developing underwater passive sensing for perceiving surrounding flows and disturbances of AUVs. The dome-shaped ISOs in crocodiles have evolved to be highly efficient receptors to sense both the direction and magnitude of flows and oscillating disturbances.

The efforts to replicate these mechanoreceptors as the sensing elements for AUVs to perceive all flows in its vicinity have shown encouraging results. By strategically arranging the artificial SA and RA domes on the surface of an AUV, an optimal sensing strategy to detect the surrounding flows would lead to a more efficient system. The work done serves as the basis for future developments to carry out quantitative analysis to establish a correlation between the stimulus and sensitivity of the dome-shaped sensors. This analysis can be useful in predicting the direction and the source of stimulus based on artificial intelligence algorithms. In doing so, the resolution of directionality detection needs to be enhanced to achieve this objective.

Taking inspirations from seal vibrissae have led several researchers in developing artificial whisker-like sensory systems to mimic the highly sensitive whiskers of the seals to detect water disturbances and track hydrodynamic trails. Various methods and architectures have been proposed, and without a doubt, each has its own advantages and drawbacks. Further work in optimizing the geometry of the artificial whiskers to reduce vortex-induced vibrations needs to be investigated to enhance the sensitivity in low flow rates. Although the underlying principles of the sensory systems in animals are not fully understood, scientists and engineers have begun to explore the mechanisms supporting its advanced capabilities and to distinguish the features of incoming signal characteristics that support wake detection similar to the wake information received and used by the seals. With this information, further development of the hydrodynamic sensory systems can achieve much more than just basic detection of hydrodynamic events.

Acknowledgments This research is supported by the National Research Foundation (NRF) Singapore under its Campus for Research Excellence and Technological Enterprise program. The Center for Environmental Sensing and Modeling (CENSAM) is an interdisciplinary research group of the Singapore-MIT Alliance for Research and Technology (SMART).

References

1. Triantafyllou, M. S., Weymouth, G. D., & Miao, J. (2016). Biomimetic survival hydrodynamics and flow sensing. *Annual Review of Fluid Mechanics, 48*, 1–24. https://doi.org/10.1146/annurev-fluid-122414-034329.
2. Windsor, S. P., Norris, S. E., Cameron, S. M., et al. (2010). The flow fields involved in hydrodynamic imaging by blind Mexican cave fish (Astyanax fasciatus). Part I: Open water and heading towards a wall. *The Journal of Experimental Biology, 213*, 3819–3831. https://doi.org/10.1242/jeb.040741.
3. Windsor, S. P., Norris, S. E., Cameron, S. M., et al. (2010). The flow fields involved in hydrodynamic imaging by blind Mexican cave fish (Astyanax fasciatus). Part II: Gliding parallel to a wall. *The Journal of Experimental Biology, 213*, 3832–3842. https://doi.org/10.1242/jeb.040790.
4. Soares, D. (2002). An ancient sensory organ in crocodilians. *Nature, 417*, 241–242. https://doi.org/10.1038/417241a.
5. Dehnhardt, G., Mauck, B., Hanke, W., & Bleckmann, H. (2001). Hydrodynamic trail-following in harbor seals (Phoca vitulina). *Science (80-), 293*, 102–104. https://doi.org/10.1126/science.1060514.

6. Fish, F. E., Howle, L. E., & Murray, M. M. (2008). Hydrodynamic flow control in marine mammals. *Integrative and Comparative Biology, 48*, 788–800.
7. Yanase, K., Herbert, N. A., & Montgomery, J. C. (2012). Disrupted flow sensing impairs hydrodynamic performance and increases the metabolic cost of swimming in the yellowtail kingfish, Seriola lalandi. *The Journal of Experimental Biology, 215*, 3944–3954. https://doi.org/10.1242/jeb.073437.
8. Yanase, K., & Saarenrinne, P. (2015). Unsteady turbulent boundary layers in swimming rainbow trout. *The Journal of Experimental Biology, 218*, 1373–1385. https://doi.org/10.1242/jeb.108043.
9. Montgomery, J. C., Baker, C. F., & Carton, A. G. (1997). The lateral line can mediate rheotaxis in fish. *Nature, 389*, 960–963. https://doi.org/10.1038/40135.
10. Montgomery, J. C., Coombs, S., & Baker, C. F. (2001). The mechanosensory lateral line system of the hypogean form of Astyanax fasciatus. *Environmental Biology of Fishes, 62*, 87–96.
11. Montgomery, J., Coombs, S., & Halstead, M. (1995). Biology of the mechanosensory lateral line in fishes. *Reviews in Fish Biology and Fisheries, 5*, 399–416. https://doi.org/10.1007/BF01103813.
12. Bora, M., Kottapalli, A. G. P., Miao, J., & Triantafyllou, M. (2017). Sensing the flow beneath the fins. *Bioinspiration & Biomimetics*. https://doi.org/10.1088/1748-3190/aaa1c2.
13. DIJKGRAAF, S. (1963). THE FUNCTIONING and SIGNIFICANCE OF THE LATERAL-LINE ORGANS. *Biological Reviews, 38*, 51–105. https://doi.org/10.1111/j.1469-185X.1963.tb00654.x.
14. Peleshanko, S., Julian, M. D., Ornatska, M., et al. (2007). Hydrogel-encapsulated microfabricated haircells mimicking fish cupula neuromast. *Advanced Materials, 19*, 2903–2909. https://doi.org/10.1002/adma.200701141.
15. Anderson, K. D., Lu, D., McConney, M. E., et al. (2008). Hydrogel microstructures combined with electrospun fibers and photopatterning for shape and modulus control. *Polymer (Guildf), 49*, 5284–5293. https://doi.org/10.1016/j.polymer.2008.09.039.
16. McConney, M. E., Chen, N., Lu, D., et al. (2009). Biologically inspired design of hydrogel-capped hair sensors for enhanced underwater flow detection. *Soft Matter, 5*, 292–295. https://doi.org/10.1039/B808839J.
17. Kottapalli, A. G. P., Bora, M., Asadnia, M., et al. (2016). Nanofibril scaffold assisted MEMS artificial hydrogel neuromasts for enhanced sensitivity flow sensing. *Scientific Reports, 6*, 19336. https://doi.org/10.1038/srep19336.
18. Kottapalli, A. G. P., Asadnia, M., Miao, J., & Triantafyllou, M. (2015). Soft polymer membrane micro-sensor arrays inspired by the mechanosensory lateral line on the blind cavefish. *Journal of Intelligent Material Systems and Structures, 26*, 38–46. https://doi.org/10.1177/1045389X14521702.
19. Asadnia, M., Kottapalli, A. G. P., Miao, J., et al. (2015). Artificial fish skin of self-powered micro-electromechanical systems hair cells for sensing hydrodynamic flow phenomena. *Journal of the Royal Society, Interface, 12*, 20150322. https://doi.org/10.1098/rsif.2015.0322.
20. Coombs, S. (2001). Smart skins: Information processing by lateral line flow sensors. *Autonomous Robots, 11*, 255–261. https://doi.org/10.1023/A:1012491007495.
21. Windsor, S. P., & McHenry, M. J. (2009). The influence of viscous hydrodynamics on the fish lateral-line system. *Integrative and Comparative Biology, 49*, 691–701. https://doi.org/10.1093/icb/icp084.
22. McConney, M. E., Anderson, K. D., Brott, L. L., et al. (2009). Bioinspired material approaches to sensing. *Advanced Functional Materials, 19*, 2527–2544. https://doi.org/10.1002/adfm.200900606.
23. Coombs, S., & Van Netten, S. (2005). The hydrodynamics and structural mechanics of the lateral line system. *Fish Physiology, 23*, 103–139.
24. Tao, J., & Yu, X. B. (2012). Hair flow sensors: From bio-inspiration to bio-mimicking—A review. *Smart Materials and Structures, 21*, –113001. https://doi.org/10.1088/0964-1726/21/11/113001.

25. Leitch, D. B., & Catania, K. C. (2012). Structure, innervation and response properties of integumentary sensory organs in crocodilians. *The Journal of Experimental Biology, 215*, 4217–4230. https://doi.org/10.1242/jeb.076836.
26. Dehnhardt, G., Mauck, B., & Bleckmann, H. (1998). Seal whiskers detect water movements [6]. *Nature, 394*, 235–236.
27. Williamson, C. H. K., & Govardhan, R. (2004). VORTEX-INDUCED VIBRATIONS. *Annual Review of Fluid Mechanics*. https://doi.org/10.1146/annurev.fluid.36.050802.122128.
28. Beem, H., Liu, Y., Barbastathis, G., & Triantafyllou, M. (2014). Vortex-induced vibration measurements of seal whiskers using digital holography. Ocean 2014 – Taipei. https://doi.org/10.1109/OCEANS-TAIPEI.2014.6964469.
29. Hanke, W., Witte, M., Miersch, L., et al. (2010). Harbor seal vibrissa morphology suppresses vortex-induced vibrations. *The Journal of Experimental Biology, 213*, 2665–2672. https://doi.org/10.1242/jeb.043216.
30. Beem, H. R., & Triantafyllou, M. S. (2015). Wake-induced "slaloming" response explains exquisite sensitivity of seal whisker-like sensors. *Journal of Fluid Mechanics*. https://doi.org/10.1017/jfm.2015.513.
31. Yang, Y., Chen, J., Engel, J., et al. (2006). Distant touch hydrodynamic imaging with an artificial lateral line. *Proceedings of the National Academy of Sciences of the United States of America, 103*, 18891–18895. https://doi.org/10.1073/pnas.0609274103.
32. Chen, N., Tucker, C., Engel, J. M., et al. (2007). Design and characterization of artificial haircell sensor for flow sensing with ultrahigh velocity and angular sensitivity. *Journal of Microelectromechanical Systems, 16*, 999–1014. https://doi.org/10.1109/JMEMS.2007.902436.
33. Bora, M., Kottapalli, A. G. P., Miao, J. M., & Triantafyllou, M. S. (2017). Fish-inspired self-powered microelectromechanical flow sensor with biomimetic hydrogel cupula. *APL Materials, 5*. https://doi.org/10.1063/1.5009128.
34. Paull, L., Saeedi, S., Seto, M., & Li, H. (2014). AUV navigation and localization: A review. *IEEE Journal of Oceanic Engineering, 39*, 131–149. https://doi.org/10.1109/JOE.2013.2278891.
35. Scalabrin, C., Marfia, C., & Boucher, J. (2009). How much fish is hidden in the surface and bottom acoustic blind zones? *ICES Journal of Marine Science, 66*, 1355–1363.
36. Kanhere, E., Wang, N., Kottapalli, A. G. P., et al. (2016). Crocodile-inspired dome-shaped pressure receptors for passive hydrodynamic sensing. *Bioinspiration & Biomimetics, 11*. https://doi.org/10.1088/1748-3190/11/5/056007.
37. Stocking, J. B., Eberhardt, W. C., Shakhsheer, Y. A., et al. (2010). A capacitance-based whisker-like artificial sensor for fluid motion sensing. In *Proceedings of IEEE Sensors* (pp. 2224–2229). Kona, HI, USA: IEEE.
38. Eberhardt, W. C., Shakhsheer, Y. A., Calhoun, B. H., et al. (2011). A bio-inspired artificial whisker for fluid motion sensing with increased sensitivity and reliability. In *Proceedings of IEEE Sensors* (pp. 982–985). Limerick, Ireland: IEEE.
39. Valdivia, Y., Alvarado, P., Subramaniam, V., & Triantafyllou, M. (2012). Design of a bio-inspired whisker sensor for underwater applications. In *Proceedings of IEEE sensors*. Taipei, Taiwan: IEEE.
40. Alvarado, P. V., Subramaniam, V., & Triantafyllou, M. (2013). Performance analysis and characterization of bio-inspired whisker sensors for underwater applications. In *IEEE International Conference on Intelligent Robots and Systems* (pp. 5956–5961). Tokyo, Japan: IEEE.
41. Eberhardt, W. C., Wakefield, B. F., Murphy, C. T., et al. (2016). Development of an artificial sensor for hydrodynamic detection inspired by a seal's whisker array. *Bioinspiration & Biomimetics, 11*, 056011. https://doi.org/10.1088/1748-3190/11/5/056011.
42. Kottapalli, A. G. P., Asadnia, M., Hans, H., et al. (2014). Harbor seal inspired MEMS artificial micro-whisker sensor. In *Proceedings of the IEEE international conference on micro electro mechanical systems (MEMS)*. San Francisco, USA: IEEE.
43. Kottapalli, A. G. P., Asadnia, M., Miao, J. M., & Triantafyllou, M. S. (2015). Harbor seal whisker inspired flow sensors to reduce vortex-induced vibrations. In *Proceedings of the IEEE international conference on micro electro mechanical systems (MEMS)*. Estoril, Portugal: IEEE.